Reaction Path Analysis of CO_2 Reduction to Methanol through Multisite Microkinetic Modelling over Cu/ZnO/Al$_2$O$_3$ Catalysts

Anže Prašnikar*, Damjan Lašič Jurković, Blaž Likozar*

Department of Catalysis and Chemical Reaction Engineering, National Institute of Chemistry, Ljubljana 1001, Slovenia

* Corresponding authors at: Department of Catalysis and Chemical Reaction Engineering, National Institute of Chemistry, Ljubljana 1001, Slovenia.

E-mail addresses: anze.prasnikar@ki.si (A. Prašnikar), blaz.likozar@ki.si (B. Likozar).

ABSTRACT

The changing hierarchical structure of the applied heterogeneous $Cu/ZnO/Al_2O_3$ material during methanol synthesis reactions hinders an efficient engineered process condition optimization, causing sub-optimal functional performance. A robust literature comparison is conducted to determine that activity is tightly coupled with Cu–Zn interactions. In order to investigate this physical behaviour further, characteristic experimental data is acquired through the catalytic reactor tests with an activated commercial catalyst, aged at different input measurements, monitored and characterized by the Brunauer–Emmett–Teller (BET), X-ray diffraction (XRD), scanning transmission electron microscopy (STEM) with energy dispersive X-ray spectroscopy (EDS), X-ray photoelectron spectroscopy (XPS), H_2 transient adsorption (TA) and N_2O pulsed surface oxidation (PSO) methodologies. It is shown that apparent rate law, exponents and activation energies do not vary significantly by increasing the ZnO_X coverage from 7% to 23%, while not all of ZnO_X over-layer is catalytically active. For $Cu/ZnO/Al_2O_3$ with ZnO_X over 7%, a highly-dispersed Al_2O_3 decreases the measured intrinsic kinetics of the Cu–Zn site, implying a steric hindrance effect. Finally, building on unveiled chemical relations, a thorough multisite system micro-kinetic model, based on systematic contribution analysis, mechanisms and quantitative density functional theory (DFT) constants is developed. Values were optimized using the sequential screening results for an industrially relevant application (the temperatures of 160–260 °C, 50 bar pressure, 12,000–200,000 h^{-1} gas hourly space velocity (GHSV) flow and relative feed compositions). Designed mathematical relationships can therefore be utilised to accurately predict the turnover, selectivity and stability/deactivation in correspondence to ZnO_X over Cu.

Abbreviations: CuZnAl, $Cu/ZnO/Al_2O_3$; CERRES, Chemical Reaction and Reactor Engineering Simulations; CSTR, Ideally mixed continuous stirred-tank reactor model; CuAl, Cu/Al_2O_3; CuSi, Cu/SiO_2; CuZn, Cu/ZnO; DFT, density function theory; GC, gas chromatography; NP(s), nanoparticle(s); PFR, plug flow reactor model; rp, reaction pathway; STEM, scanning transmission electron microscopy; STM, Scanning tunnelling microscopy; TCD, thermal conductivity detector; TOF, turnover frequency; XPS, X-ray photoelectron spectroscopy; XRD, X-ray diffraction

1. Introduction

In the recent decades, the global concentrations of greenhouse gases have increased significantly, posing a serious threat to the human society. The major actors in this regard are CH_4 and CO_2, and unfortunately their emissions don't seem to be declining. On the contrary, as the population grows and humanities' energy needs are increasing, it would seem naive to expect the emissions to significantly drop in the near future. For this reason, appropriate technologies for the capture and utilization of the emitted gases, either at the source or from the atmosphere, are highly sought-after, and there has been a significant increase in research focus related to them. Catalytic conversion of carbon dioxide into value added products is an example of such a promising technology. Specifically, methanol synthesis can be incorporated as a tool for utilization of CO_2 emissions on a large scale,[1] in particular, by using renewable or surplus electricity for hydrogen generation.

The methanol synthesis reaction is generally performed at high pressures (>20 bar) and moderate temperatures (180-300 °C), due to the methanol being thermodynamically favorited at these conditions. As with most industrially relevant gas-phase processes, methanol hydrogenation requires a catalyst to achieve sufficient efficiency. Different metal-based catalysts were studied for this process, including Cu[2], Pd[3] and Au[4]. The most appropriate seem to be catalysts derived from the CuZnAl system ($Cu/ZnO/Al_2O_3$) due to its welcome combination of low price, high activity and high stability at the aforementioned conditions. That's why the CuZnAl catalyst is used in the typical commercial methanol synthesis plant. CuZnAl has been extensively studied by investigation of catalyst synthesis methods[5–12], model catalytic systems[13–18] and advanced characterization methods[19–22]. *Ab initio* methods were applied to extend the knowledge about the reaction mechanism.[13,23–29] Furthermore, selectivity toward CO, MeOH, CH_4 or even EtOH can

be extracted from scaling relations of binding energies of intermediates to select optimal catalytic system for the direct conversion of CO [30,31] or CO_2.[32]

Efficient optimization or modification of the process is achieved on the basis of detailed understanding of the interaction between catalyst material and reaction species. In particular for the CuZnAl case, the intimate contact of Cu and ZnO phases is responsible for the major part of methanol synthesis. The most linear relationship between measured number of active sites and activity is achieved by using N_2O decomposition methods, where we measure not only surface copper sites but also partially reduced ZnO. Cu/ZnO catalysts can form the Cu-Zn alloy during exposure to reductive conditions, although the exact structure of actively present Zn during catalysis is still debatable.[13] The condition-sensitive nature of the Cu-Zn contact is responsible for the growth of separate Cu and ZnO regions in oxidative environment[33,34] and an increase in Cu-Zn contact under reductive conditions[20,35]. Long-term exposure of the catalyst to the reaction conditions leads to ZnO_X overlapping over Cu NPs, causing partial deactivation.[21,36] The activity for methanol synthesis increases with increasing Zn coverage over Cu to a point, as identified by testing Zn decorated Cu single crystal planes[13,14] and industrial CuZnAl catalyst.[37] The amount of Zn in close contact with copper atoms on the surface is therefore an important factor and is pointing to the synergy of the system between the ability of the Cu phase to activate H_2 and of the Zn phase to increase the stability of reaction intermediates and promote the subsequent hydrogenation to produce methanol.

In present work, we focus on the identification of important parameters affecting the catalytic activity of commercial CuZnAl catalysts by means of structure (and composition)-activity relations connecting the catalyst's features with functions. The behaviour of catalysts with different ZnO_X morphologies, prepared by exposing them to different gas compositions and investigated in detail in our previous work,[33] is compared and used to prepare an adequate

model for practical applications. Furthermore, the multisite microkinetic model, defined by integrating the structure-activity relationships with the reaction mechanism obtained from *ab initio* calculations, is refined using the results of industrial CuZnAl catalysts and validated by comparing its output with the results of Zn coverage variation experiments and published catalytic tests at various conditions, indicating a high predictive power.

2. Methods

2.1. Experimental

2.1.1. Materials

The catalytic material used was a commercial CuZnAl catalyst (HiFuel W230, Alfa Aesar) with particle size between 240 and 400 μm. The catalyst contained 50.2 wt % of CuO, 30.8 wt % of ZnO, and 18.7 wt% of Al_2O_3 and graphite as a binder. The CuZnAl catalyst was aged and extensively characterized in our previous work.[33] Aging was performed in various gas compositions including pure H_2, H_2/CO_2 mixture at low, medium and equilibrium conversion, H_2/H_2O mixture and $H_2/CO_2/H_2O$ mixture. The gases used for catalytic testing were pure H_2 (99.999%, Messer), CO_2 (99.999%, Messer) and CO (99.999%, Messer).

2.1.2. Catalytic reaction testing

In this work we performed two sets of catalytic testing. The first was used to compare the activity trends of the samples with low Zn coverage (R4, aged at low conversion[33]) and high Zn coverage (R3, aged at equilibrium conversion[33]). To obtain apparent reaction orders and apparent activation of relevant reactions energies for both samples, we varied inlet gas composition (at 240°C, 20 bar) and temperature (at one gas composition). The catalytic tests were performed in a parallel packed bed reactor, with tube diameter 6.35 mm, connected via heated line to gas chromatograph (Agilent 490 Micro GC, TCD detectors equipped with

CP-Molsieve and PoraPlot U columns.). Various gas compositions were attained by mixing the aforementioned pure gases.

The second set is a conditions screening for the modelling purposes. Before the testing, the CuZnAl catalyst was reduced at 300 °C for 12 h in H_2 at 1 bar and aged at 260 °C, 50 bar, H_2/CO_2=3 for 12 h, at equilibrium conversion to obtain stable and consistently active catalyst with high Zn coverage to imitate catalyst in long term methanol synthesis campaign (sample designated as R9). Catalytic testing was performed at a high pressure of 50 bar using 57 different sets of conditions varying in temperature (160 °C-260 °C), inlet gas compositions (various ratios of H_2, CO_2 and CO), and three different gas flow rates. The table of the reaction conditions can be found in Supporting Information, Table S1. Additionally, various tests with different catalyst particle sizes and different flow rates were conducted to show the absence of any mass transport limitations. Isothermal reactor behaviour was also demonstrated by measuring the temperature at different points the catalyst bed. These results are included and discussed in Supporting Information, Chapter S11.

2.1.3. Characterization

N_2O pulse chemisorption was performed using Micromeritics Autochem II 2920 with 100 mg of catalyst sample. Firstly, the samples were purged in 5% H_2/Ar at 240 °C for 30 min, followed by N_2O pulse chemisorption at 50 °C. The N_2O gas (Messer) decomposition was monitored with a daily calibrated mass spectrometer Pfeiffer Vacuum Thermostar (m/z = 28 and 30). The method is used to measure the number of Cu surface atoms and was validated by H_2 transient adsorption.[33] The catalysts samples (R1-R8) were previously analysed by XRD, H_2 transient adsorption, STEM, XPS, N_2 physisorption which are described in detail in our previous study.[33]

2.2. Theoretical methods

2.2.1. Multisite microkinetic modelling

The reaction model was based on DFT reaction rate constants by Kattel et al.[13] for Zn/Cu(211) surface and the measured kinetics of H_2 adsorption and desorption on Cu.[38] The full reaction network is included in Supporting information, Table S2. The reaction rate for each pathway and the total species consumption/generation were computed as shown in equations 1 and 2.

$$r_n = k_{forward} \prod_{i=1}^{I} \theta_i^{S_{i,n,forward}} - k_{reverse} \prod_{j=1}^{I} \theta_j^{S_{j,n,reverse}} \tag{1}$$

$$\frac{d\theta_i}{dt} = R_i = \sum_{n=1}^{N} (-S_{i,n,forward} + S_{i,n,reverse}) r_n \tag{2}$$

In equations 1 and 2, r_n is the rate of the n-th reaction, $k_{forward}$ and $k_{reverse}$ are the forward and reverse reaction rate constants, θ_i is the surface coverage of species i (dimensionless), $S_{i,n,forward}$ and $S_{i,n,reverse}$ are the stoichiometric amounts of the species in the reaction, I and N are the number of species and reactions, respectively.

For the reactor transport model, two different models were compared: Ideally mixed continuous stirred-tank reactor (CSTR) model and a plug flow reactor (PFR) model which included both convective and dispersive (molecular diffusion) mass transport. The overall mass balance equations for both reactor types are shown below (Eq. 3 and 4).

$$CSTR: \quad \frac{dC_i}{dt} = \frac{v_{ax.}}{L} \left(C_{i,inlet} - C_i \right) + C^* \frac{1-\varepsilon}{\varepsilon} R_i \tag{3}$$

$$PFR: \quad \frac{\partial C_i}{\partial t} = -v_{ax.} \frac{\partial C_i}{\partial x} + \frac{D_i}{\tau} \frac{\partial^2 C_i}{\partial x^2} + C^* \frac{1-\varepsilon}{\varepsilon} R_i \tag{4}$$

In equations 3 and 4, t and x represent the temporal and lateral dimensions of the reactor, respectively, while i denote the species. $v_{ax.}$ is the superficial gas velocity in the axial (length-wise) direction of the reactor, L is the reactor length, C_i and $C_{i,inlet}$ are the gas phase and inlet concentrations of species i, R_i is the sum of all reaction terms for species i. D_i is the diffusivity of species i, τ is the tortuosity factor with the assumed value of 1.5, as seen often in literature[39,40], and ε is the void fraction assumed to be 0.4.[39,40] C^* is the total concentration of active sites per volume of the catalyst.

As the calculated Péclet number was approximately 1 for our system, it would seem the axial diffusion would provide adequate mixing for any axial gradient to be negligible. This was confirmed by comparing the reactor models in the range of operating conditions, as seen in Supporting information (Section 8), which yielded nearly identical results. Therefore, the CSTR model was used for all the modelling in this study in order to achieve faster computing times. Furthermore, both intra- and extra-particle mass transport limitations were neglected in the model. This was previously confirmed by calculations for our testing rig for methanol synthesis.[41] Furthermore, we've conducted thorough tests for both types of mass transport as well as for the isothermal behaviour of the reactor (Supporting Information, Chapter S11), which prove that these simplifications can be applied.

All the reactor modelling, parameter optimization and sensitivity analysis calculations were performed using the CERRES software.[42] Other areas of model development are discussed in Section "3.2 Multisite microkinetic model definition".

3. Results and discussion

3.1. Composition-activity relations

Typical methanol synthesis catalyst consists of Cu, Zn and Al forming different compounds, depending on the preparation and treatment. To obtain the knowledge about structural and compositional effect in a holistic manner we first review turnover frequencies (TOF) of catalyst activities with different compositions ($Cu_xZn_yAl_zSi_{1-x-y-z}$) for MeOH synthesis and present them as TOF ratios (Table 1) between catalysts reported in each study.[5–7,9,10,43–45] The comparison of TOF(MeOH) ratios between samples reported in a single study provides maximally consistent results, robust in terms of the characterization conditions changes between different works. Reaction temperature, proximity to chemical equilibrium, copper surface area determination and other relevant parameters for TOF ratios calculations can be found in Supporting Information, Table S3.

Table 1: The comparison of TOF ratios of Cu-Zn-Al-Si systems obtained from different studies.

Source	TOF (MeOH) ratio [/]					
	$\dfrac{CuZn}{CuSi}$	$\dfrac{CuZnAl}{CuSi}$	$\dfrac{CuAl}{CuSi}$	$\dfrac{CuZnAl}{CuAl}$	$\dfrac{CuZn}{CuAl}$	$\dfrac{CuZnAl}{CuZn}$
Van den Berg [5]	10	-	-	-	-	-
Fujitani et al.[6]	16-27	-	-	-	-	-
Günther et al. [7]	>10	-	-	-	-	-
Fujitani et al. [43]	4	3.4-4.5	2.7	1.3-1.6	1.5	0.97
Kurtz et al. [10]	-	-	-	1.9-2.8	1.5-1.7	1.5
Saito et al. [44]	8.1	-	3	2.7	-	-
Schumann et al.[9]	-	-	-	-	-	1.3
Behrens et al.[45]	-	-	-	-	-	0.95

Composition severely affects the activity as can be seen from Table 1. The TOF ratios between different studies also vary to some extent. To obtain a direct comparison between intrinsic activities of all investigated catalysts, we performed a regression constrained by the TOF ratios as an output. In this manner we present intrinsic activities for MeOH synthesis of all materials on the same scale. The average relative TOF(MeOH) can be found in Figure 1. Error bars represent the largest deviations of TOF ratios from the average relative TOF value, caused by different preparation, testing conditions and characterization methods. Additional information about relative TOF(MeOH) and error bar estimation can be found in Supporting Information, Section 4. In spite of different conditions, we can still clearly observe that the activity normalized to the copper surface increases in following order: CuSi<CuAl<CuZn≈CuZnAl.
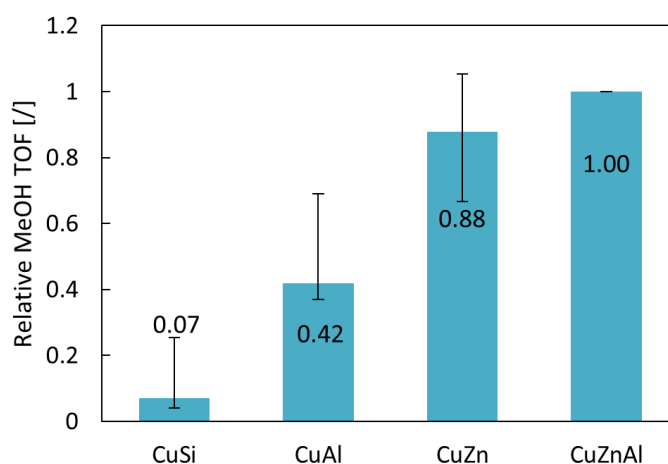

Figure 1: The overview of TOF relations obtained for synthesis of MeOH from $CO_2/CO/H_2$ mixtures between 200°C -260 °C. The error bars represents the largest deviations from the ratio of optimized TOF.

Copper deposited on SiO_2 catalyses the reaction very poorly. Al_2O_3 increases the relative intrinsic activity between 1.6 to 6.7 times compared to pure copper (Cu/SiO_2). All of the catalysts in this study were synthesized by co-precipitation of Cu and Al phases which means that Al_2O_3 is finely dispersed over the Cu surface and can therefore increase the activation of

CO_2.[43] The intrinsic activity of the bimetallic Cu/ZnO catalyst is larger by a factor of 3.5 to 22 compared to the activity of copper surface (Cu/SiO$_2$). As evidenced by several studies, the Cu-ZnO catalyst forms a Cu-Zn surface alloy, evidenced by STM, XRD and XPS studies,[17,34,46] enabling high utilization of the copper phase due to good Cu-Zn contact. The unit cell size of Cu crystallite found in Figure 2 is also an evidence of the CuZn alloy. By adding the complexity of the industrial catalyst, we observe that the copper surface of the CuZnAl catalyst is 4-25 times more active than pure copper nanoparticles, although a 14% higher average activity compared to copper on CuZn is insignificant. The most important role of the Al$_2$O$_3$ phase is that it acts as a refractory material which separates Cu and ZnO particles and provides a high surface area catalyst.[10,33] Higher Zn coverage over Cu is obtained using smaller ZnO NPs, and subsequently a higher apparent TOF. Additionally, an increase in absolute activity was observed previously when small amounts of Al was added, which was caused by the doping of ZnO and the subsequent higher Zn coverage over Cu surface[9]. As observed for the CuAl catalyst, the addition of Al$_2$O$_3$ also increases the activity of the copper surface, although it can stabilize Zn in a form of ZnAl$_2$O$_4$, reducing the availability for the reaction catalysis as in the case of Zn-silicate[5]. As seen from this overview, the CuZn synergy and Al$_2$O$_3$ contribution play a highly significant role. Furthermore, the activity is also dependent on the phase structures and distribution, which is covered in the next section.

3.2. Structure-activity relations

3.2.1. Cu/ZnO interphase or Zn/Cu as a model structure

Two types of CuZn model catalyst activities were reported which present two extremes of Cu-Zn contact; Cu/ZnO(0001)[13,15] and an inverse catalyst Zn/Cu(111)[13,14]. Identification

of the appropriate system is crucial for the microkinetic model definition. This is tackled below by a description of Zn dynamic behaviour and catalytic tests.

Zn in CZA catalyst is in the form of ZnO after calcination. During reduction it can be partially reduced and migrate over Cu[37]. After a long term exposure to reaction conditions, the ZnO forms an overlayer and decreases the activity.[36] Additionally, STM study observed agglomeration of Zn deposited on Cu(111) after oxidation.[34] The catalyst's activity is generally correlated by the quantity of the consumed N_2O[10,47,48], which corresponds to the copper surface and oxygen vacancies due to Zn surface atoms. The fact that a structure-activity relation is observed is due to the same prereduction and similar catalyst morphology, which could provide consistent Zn distribution over Cu NPs.[37] Normalization of the catalyst's activity to purely copper surface does not provide such structure activity correlations for CuZn catalysts, since Zn atoms replace copper atoms on the surface[49] and are also the sites which facilitate the conversion of surface-bound carbonaceous intermediates. The changing nature of ZnO_X morphology during a shift in environmental conditions hinders a more detailed knowledge about the active site, which is crucial for the selection of a model structure.

In the work by Fujitani et al.[50] it was observed by that adding ZnO/SiO_2 to Cu/SiO_2 by physical mixing, the catalyst becomes up to 4-times more active after reduction and the activity stays the same after Zn/SiO_2 is removed. The lattice constant of copper increases due to incorporation of up to 13% Zn into Cu NPs, leading to brass formation. In our previous work,[33] we modified a highly active CZA catalyst by exposure to various gas mixtures and observed that CO/MeOH causes ZnO overgrowth over Cu while H_2O causes separate growth of ZnO and Cu NPs. Copper unit cell size was additionally determined by the examination of XRD diffractograms and presented as Zn content in Cu NPs using correlation [51](Figure 2). We found out that after reduction at 300 °C/12 h (1 bar H_2), the Cu phase contains on the

average 8% of Zn in the Cu crystallite, while further aging in gas mixture with a high H_2O/H_2 ratio causes the migration of Zn to the surface, leaving only 3% of Zn in Cu. The surface Zn is stabilized by the CuZn alloy found in oxidative environment[18] as well as by the reaction intermediates in methanol synthesis.[14] The reaction intermediates are unable to decrease the Zn content inside the Cu NPs despite the fact that they stabilize it on the surface. H_2O promotes ZnO particle growth[33] and could increase mobility of surface Zn from the Cu onto the ZnO phase, resulting in a Zn free copper surface. CO and/or MeOH act in contrary fashion; increasing the Cu-Zn contact causes Zn migration from ZnO to Cu.[33] The Zn surface concentration on Cu therefore increases with proximity to the ZnO NPs due to two competing processes during reaction conditions. The question is whether a lower activity of Zn sites with smaller number of neighbouring Cu atoms could be observed. If the activity of separated Zn atoms with Cu atoms is indeed much higher than the activity of aggregated Zn atoms, it is therefore more suitable to use Zn/Cu(111) as the model structure instead of Cu/ZnO(0001).
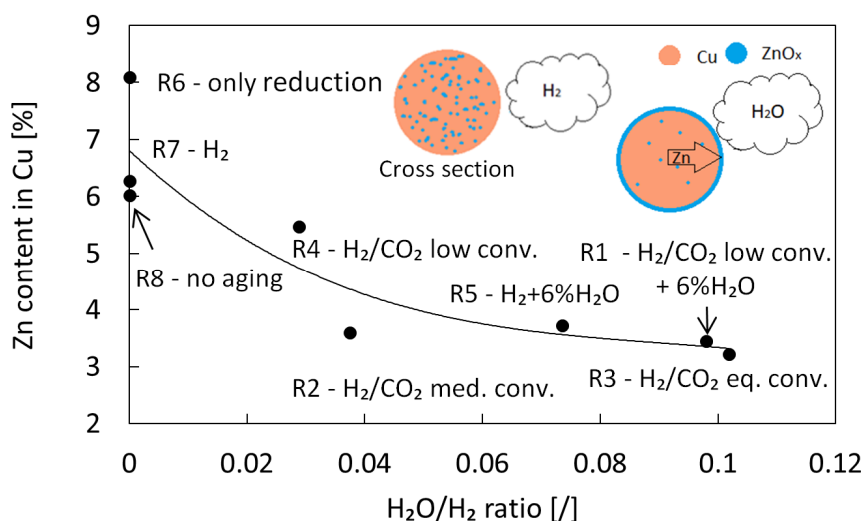

Figure 2: The Zn content in the bulk Cu NPs in dependence of H_2O/H_2 ratio in the aging composition. The Cu unit cell size of sample R6 is equal to 0.3632 nm while 0.3615 nm is the pure Cu unit cell size.

The activities of Cu/ZnO(0001)[13,15] and Zn/Cu(111)[13,14] model catalyst systems at 550 K, $p(H_2)$=4.5 bar and $p(CO_2)$=0.5 bar are compared. Since the intrinsic activities of CuZn catalysts are generally higher than those of Cu catalysts by a factor of 10 (Figure 1), the active sites are here normalized to Zn sites which are in close contact with Cu. This is straightforward for the Zn/Cu(111) catalyst, where Zn coverage (5% coverage) is used, while for the Cu/ZnO(0001) catalyst (10% Cu coverage) we use the area fraction of single row Zn atoms around Cu NPs. Study by Koplitz using STM[52] indicated 1.5-2.5 nm Cu NPs for 10% Cu coverage on ZnO(0001). At those conditions between 21-24% of the whole surface is represented by the interphase between Zn and the Cu/ZnO(0001) catalyst. The activities are presented in Figure 3 (blue columns present the activity normalized to Zn sites, reference grey columns present absolute activities). It is observed that the Zn sites are 3.7 times more active on Zn/Cu(111) than on Cu/ZnO(0001) at 550 K. For the reference, the activity of Cu(111) at the same conditions is significantly lower. Higher normalized activity of highly Cu-coordinated Zn atoms and high Zn distribution over Cu NPs points to the fact that Zn-Cu patterns represent the most important active sites for methanol synthesis. Similar decrease of activity normalized to Zn sites was also observed in a commercial catalyst, as discussed in the following section where it's also verified if the nature (reaction orders, apparent activation energy) of the active sites changes significantly.
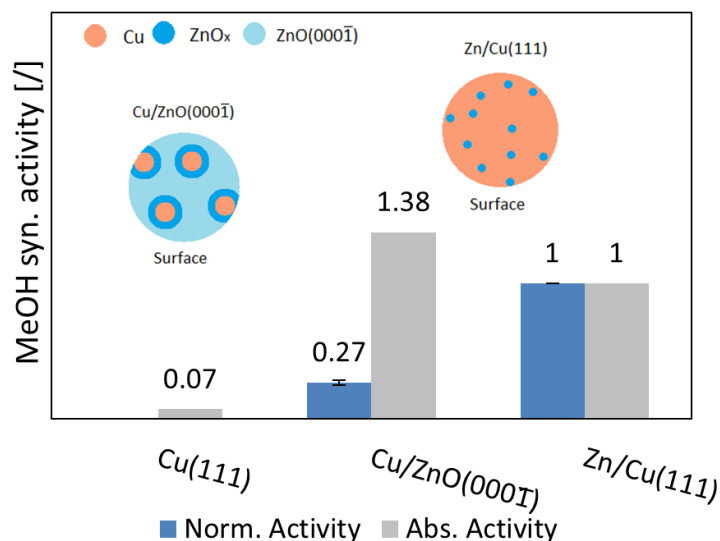
Figure 3: Comparison of model catalyst's MeOH activity[13,18] to inspect an effect of Zn-Cu structure. The error bars represent the variation of Cu NP on ZnO(0001) from 1.5 to 2.5 nm.

3.2.2. Does the behaviour of catalytic sites change significantly with morphology change?

The morphological implications on catalysis were identified on two CuZnAl catalysts which are relevant to the methanol synthesis; R4 (aged at low conversion) and R3 (aged at eq. conversion). The catalysts exhibit large differences in structure, particularly in the value of $ECSF_{Cu}$ (exposed crystallite surface fraction of Cu) as observed in our previous work.[33] Firstly, we use $ECSF_{Cu}$ to estimate the ZnO_X coverage on the copper surface of R3 and R4. The exposed Cu surface fraction is equal to 53% in the case of sample R4 and decreases mainly due to ZnO overlaying to 37%. As a reference we use the amount of Zn in bulk Cu of the sample after reduction (sample R7) which is 8.1% and equalize it with the amount of Zn on Cu at the $ECSF_{Cu}$ =52%. In this way, the calculated ZnOx coverage is 7.1% and 23% for the samples R4 and R3 respectively. The number of ZnO_X sites was approximated by using ZnO_X coverage and concentration of Cu sites as shown in equation below (Eq. 5):

$$c_{ZnOx} = c_{Cu} \frac{ZnOx\ coverage}{1 - ZnOx\ coverage} \tag{5}$$

A similar approach of Zn coverage estimation was used by Kuld et al. [37] which is here upgraded to account for the sintering of copper particles. The catalysts with low (R4) and high (R3) ZnO_X coverage were tested at different $H_2/CO_2/CO$ gas mixtures to obtain the reaction rate coefficients and orders of reactions using a power law model. For each change in reaction conditions, we performed a reaction step at standard conditions 20 bar, $H_2/CO_2=3$, 240 °C for 2 h to minimize any effect of structural change on the observed catalytic performance. All catalytic activities were normalized to the average of activities at standard conditions. The overall activity decreased only by 1.8% for R3 and 3.5% for R4 and the selectivity increased only by 1.4% for R3 and 1.3% for R4 during those tests, meaning that the surface of the samples did not change significantly. First, the coefficients for CO_2 hydrogenation were obtained for reverse gas shift reaction and methanol synthesis by using the data of CO_2/H_2 gas mixtures. Next, the coefficients for the reaction of CO to MeOH were obtained by using the data of $CO_2/CO/H_2$ mixtures, while using the previously determined coefficients for CO_2 hydrogenation. We found out that methanol is formed almost exclusively from CO_2 at 240 °C on CuZnAl catalysts as can be observed by comparing the values of reaction rate coefficients of the CO_2 to MeOH ($6.3·10^{-4}$, $3.8·10^{-4}$) and CO to MeOH (0 and $8.5·10^{-6}$) reactions. Due to a decreased water production rate when a large fraction of CO was present, we also added the water gas shift reaction and determined its coefficients. In addition, the approach to equilibrium[53] was calculated and determined that it has insignificant effect on apparent reaction coefficient determination. All the comparisons between experimental and model data along with approach to equilibrium calculations can be found in Supporting Information in Section 5. Intriguingly, all reactions could be modelled by the same reaction orders for both of the catalysts with satisfactory accuracy despite the differences in ZnO coverage and morphology, pointing to the fact that there is no significant difference in the supply of H_2 or

CO_2 to the catalytic site for CO or MeOH formation. There is, however, a difference in the reaction rate coefficients between the two catalysts as expected due to different TOF activities. Apparent activation energies decreased slightly, although the changes in MeOH synthesis are insignificant.

Table 2: Comparison of the apparent catalytic parameters of catalysts with high and low ZnO_X coverages.

Reaction	Expression	a^i	b^i	k [mol/(mol Cu·s·bar^{a+b})]^i		Ea [kJ/mol]^j	
				R4-7.1% ZnO_X cov.	R3-23% ZnO_X cov.	R4-7.1% ZnO_X cov.	R3-23% ZnO_X cov.
CO_2 to MeOH	$k\,p_{CO_2}{}^a\,p_{H_2}{}^b$	0.057	1.2	$6.3 \cdot 10^{-4}$	$3.8 \cdot 10^{-4}$	52.8 ± 4.3	47.5 ± 5.3
RWGS	$k\,p_{CO_2}{}^a\,p_{H_2}{}^b$	0.16	0.069	$1.3 \cdot 10^{-2}$	$1.0 \cdot 10^{-2}$	138.4 ± 3.2	126.2 ± 2.7
CO to MeOH	$k\,p_{CO}{}^a\,p_{H_2}{}^b$	0.74	1.4	$<5 \cdot 10^{-6}$	$8.5 \cdot 10^{-6}$	n.a.	
WGS	$k\,p_{CO}{}^a\,p_{H_2O}{}^b$	1.1	0.45	$1.7 \cdot 10^{-2}$	$1.1 \cdot 10^{-2}$		

[i] Measured at 20 bar, 240 °C at various gas compositions.

[j] Measured at 50 bar 180-240 °C, $p(H_2)/p(CO_2)$=2.5, GHSV 40,000 h^{-1}

The results of kinetic analysis for MeOH and CO formation from Table 2 are used to evaluate the effect of ZnO_X coverage. The reaction rates of methanol synthesis and RWGS reaction are normalized to the concentration of copper sites and ZnO_X sites and presented in Figure 4.
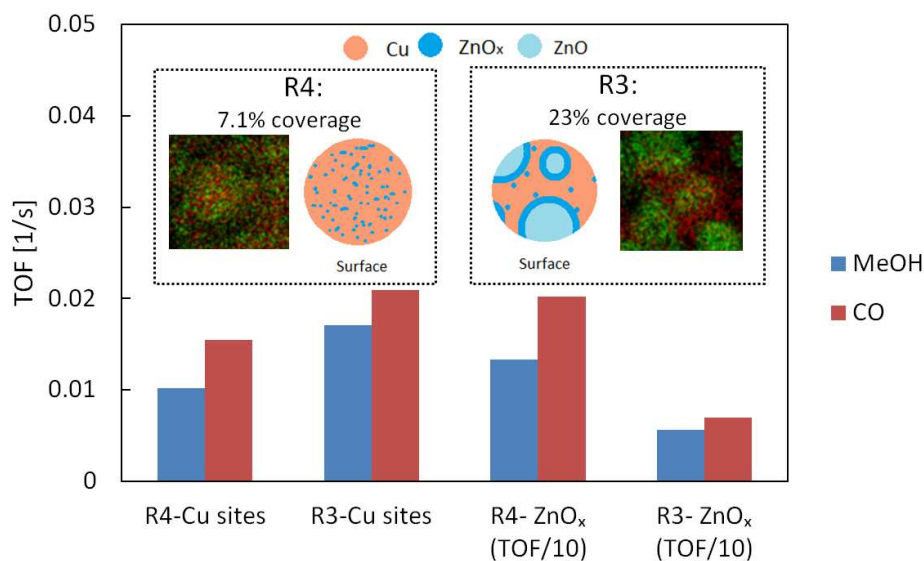
Figure 4: TOF for MeOH and CO obtained from the model at 240 °C, 20 bar, $H_2/CO_2=3$. For the TOF calculation, reaction rates are normalized to Cu sites and ZnO_X sites. The inset pictures are STEM-EDS micrographs, where green represents Cu and red ZnO_X. Full EDS images are in the Supporting Information, Section S12.

We can observe that the activity normalized to Cu sites increases with higher coverage of ZnO_X, while the activity normalized to ZnO_X sites decreases with increasing ZnO_X coverage. The increase in Cu normalized activity is assigned to a larger amount of ZnO_X on the copper surface. The decrease of ZnO_X-normalized activity is due to the agglomeration of ZnO, since all ZnO is not in close enough contact with Cu (the source of hydrogen) to proceed with hydrogenation. The deactivation by ZnO overlayer was also observed by Lunkenbein et al.[36] The long-term impact of ZnO overgrowth by assessment of a 148 day stability study[36] is discussed in Supporting Information, Section 6, where we observe constant copper normalized activity between day 50 and day 148, while exposed copper surface continually decreases. This observation additionally points to the fact that the separated Zn active sites on Cu NPs are not significantly affected by ZnO overgrowth over Cu near ZnO NPs. Due to a large difference in ZnO_X-normalized activity in the definition and use of the

microkinetic model the exclusion of inactive Zn is necessary. However, to avoid the wrong conclusion of the lower intrinsic activity being caused just by the lower apparent number of active Zn sites, Cu sites need to be included in the microkinetic model as well, in order to account for the actual hydrogen activation capability. The ZnO_X distribution over Cu does not significantly effect on the nature of catalysis (reaction orders and activation energy). The question of the effect of other phases present in the catalyst is addressed in the next section.

3.2.3. Is Zn coverage and distribution the only important factor determining the intrinsic activity in commercial CuZnAl catalysts?

The ZnO_X-Cu contact can be altered by the presence of Al_2O_3 in commercial catalysts, influencing the activity. As it is observed in Table 1 and Figure 1, the CuAl catalysts are 1.6 to 6.7 times more active than CuSi ones and the intrinsic activity of CuZnAl samples was measured to be 0.95 to 1.5 of the CuZn samples, although the boundaries of ratios are not definite. We investigated how changing the surface composition impacts the intrinsic activity (normalized to copper surface) of samples R1-R7[33] by structure-activity relations. TOF variation was connected to the difference of the $(Zn/Cu)_{XPS}$ surface composition ratio, the $(Al/Cu)_{XPS}$ surface composition ratio and the weight percentage of $ZnAl_2O_4$. Additional information about the calculation of TOF breakdown can be found in Supporting Information, Section 7. As expected, we observed that the main contributor is the Zn/Cu ratio, while the Al/Cu ratio and the weight fraction of $ZnAl_2O_4$ had a negative contribution to the activity (Figure 5). The Al_2O_3 coverage over active sites can be expected since in our case Al_2O_3 covers around 50% of the CuZnAl catalyst.[33] We imagine that the Cu-Zn atom pattern is next to the Al_2O_3 cluster which limits the supply of the adsorbed hydrogen for continuing the hydrogenation of reaction intermediates. The negative effect of $ZnAl_2O_4$ can be explained by the same reason as in the case of $CuZn/SiO_2$ where Zn is stabilized in zinc

hydroxy(phyllo)silicate and cannot bind the reaction intermediates in the same manner.[5] Al_2O_3 phase can have a negative impact on the activity of CuZn active sites, however it is in the end beneficial since it prevents sintering. The higher TOF values of CuZnAl catalysts compared to the CuZn catalyst are highly likely measured due to smaller ZnO NPs, allowing greater Zn coverage over Cu.
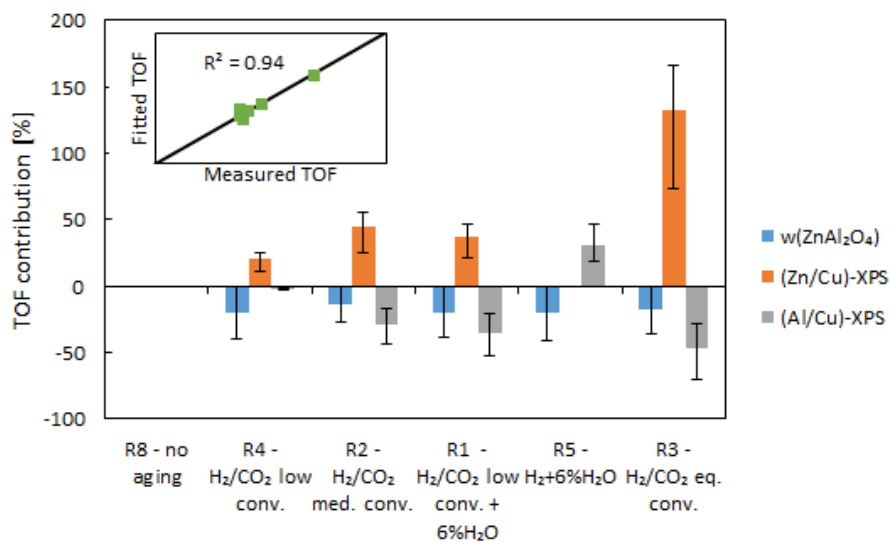

Figure 5: Contributions to the TOF by change of (Zn/Cu)-XPS, (Al/Cu)-XPS and weight percentage of spinel relative to sample R8. Error bars represent the results of parameter variation where the relative average error of TOF estimation increased from the original 4.7% to 10%. All samples are the same CuZnAl catalyst aged at different conditions. No change of TOF is attributed to the change of Zn/Cu ratio in the case catalyst aging in H_2+6% H_2O, since the ratio remains constant.

3.3. Multisite microkinetic model definition

Based on the observed structure activity relations, the most influential variable for methanol synthesis is the Zn coverage on Cu surface. As observed from the apparent reaction orders and activation energies in Table 2, the ZnO_X morphology does not significantly affect the nature of the active sites. The property that influences the activity of a CuZn catalyst the most is the catalytic availability of Zn, dispersed over Cu, as observed on Figure 4.

In this work, a multisite microkinetic model with Cu and Zn catalytic sites was developed based on the DFT reaction rate constants by Kattel et al.[13] for the Zn/Cu(211) surface, experimentally measured kinetics of H_2 adsorption and desorption,[54] catalyst characterization and catalytic conditions screening. The catalyst structure used in the DFT model[13] is consistent with observed structure-activity relations, where Zn atoms are dispersed over Cu crystal surface. Fujitani et al. performed catalytic test using Zn/Cu(111) model catalyst [14] and showed using XPS that the binding energy of Zn 2p3/2 at 0.19 ML Zn coverage is lower than binding energy at higher Zn coverage after reaction, pointing to the fact the Zn is not fully oxidized. Additional information about model structure selection and DFT model development can be found in Supporting Information, Section S2.

The site adsorption preference is developed based on the fact that H_2 is activated on Cu sites, while the carbon reaction intermediates typically occupy neighbouring Zn and Cu sites due to bidentate binding or steric hindrance.[13] All oxygen based species (O, H_2O, OH) adsorb on Zn sites due to a higher binding energy than on Cu sites.[24] Due to a higher binding energy of carbon reaction intermediates (binding energy of bidentate formate: -3.41 eV) in comparison with CO (-1.02 eV) on Zn sites and similar adsorption energy of CO on Zn (-1.02 eV) and Cu(111) (-0.99 eV[26]) sites, the adsorption of CO is limited to Cu sites. As observed in Table 2, CO conversion to MeOH is negligible, while the rate of WGS is important, where CO can react with hydroxyl species on Zn sites. The catalyst surface and binding species are drawn in Figure 6.
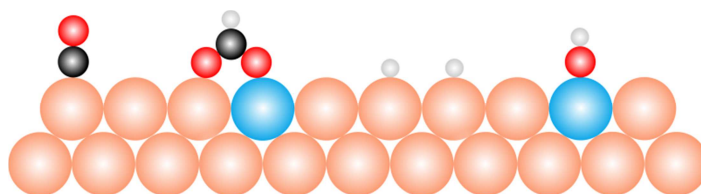

Figure 6: Adsorption of reactants and intermediates. Cu: orange, Zn: blue, O: red, C: black, H: white.

The concentration of Cu sites is obtained by N_2O pulse adsorption by prereduction at 240 °C, 0.1 bar H_2 for 1 h where ZnO reduction is negligible as proven by H_2-TA.[33] Determination of the concentration of Zn sites is more complex due to agglomeration of Zn atoms. Sample R4 is taken as a standard because of a small Zn coverage (7.1%) where Zn atoms are assumed to be completely dispersed over Cu and are therefore completely catalytically accessible. The reaction rate constants of the individual reactions are influenced by several factors which limit direct *ab initio* reaction constants application. This involves exposure of different crystal planes with different activity [13,14,55], catalyst surface morphology and composition change according to the environmental conditions resulting in changing Zn coverage[37] and the effect of adsorbate coverage on activation energy of elementary reaction steps[56]. For those reasons the parameters determined by DFT are not final and need to be optimized. We tackle this challenge by taking into account Zn coverage over Cu NPs, since is the most important variable which has not been previously implemented in any microkinetic model. Still however, the effects of the intermediate coverage on the activation energy[57] and the preexponential factor should be in the future included to obtain accurate results for high Zn coverage over Cu. Original and optimized reaction rate constants can be found in Supporting Information, Table S2.

3.4. Model validation

By initial inspection of the ZnCu(211) model of MeOH synthesis[13] using sensitivity analysis at industrially relevant conditions (240 °C, 20 bar, $CO_2/CO/H_2$ mixture), we observed that MeOH can be formed through the formate pathway (path rp1, Figure 7) faster than through the CO-hydro pathway (paths rp3+rp2). However, CO is likely being formed through the CO-hydro pathway (path rp3) rather than through the direct redox mechanism (path rp4). This observation is consistent with the fact that MeOH is largely formed from CO_2 on CuZn catalysts (Table 2). For this reasons we focused on the rate constant optimization for pathways rp1 and rp3.
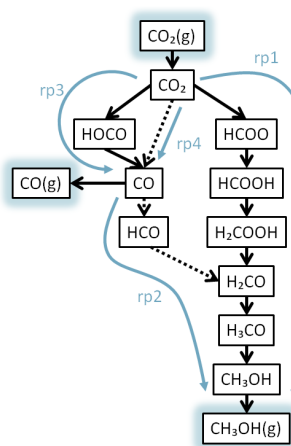

Figure 7: Reaction scheme used in our study. Black arrows represent the elementary reaction steps and blue arrows the reaction pathways. Reaction species in black squares without "(g)" are adsorbed on the catalyst's surface.

The comparison between the results of the optimized model and experimental data can be found in Figure 8 and the corresponding concentration of active sites is in Table 3. Parity plots can be found in Supporting Information Section 9. Sensitivity analysis shows a higher than linear dependence of methoxy hydrogenation (Supporting Information, Section 10). In addition, good match of model results with 118 experimental points by Park et al[58] was obtained for CuZnAl catalyst (Supporting Information, Section 13). The model constants were

optimized to describe the behaviour of catalytic tests of samples R9 and R4 at the measured concentration of Cu sites by N_2O PSO and Zn sites for the sample at low coverage R4 (7.1% Zn). The concentration of Zn sites on sample R9 was obtained by comparing the activity with the R4 sample, since the concentration of active Zn sites cannot be determined accurately for the catalyst aged at equilibrium condition due to Zn phase agglomeration. Also the Zn concentration of the R3 sample with observed high coverage was fitted due to an observed activity which was lower than expected for 23% coverage and it was computed that the copper surface is covered by 13.1% of active Zn. As mentioned before, we observed that the morphology difference between the catalysts R3 and R4 does not significantly affect the apparent reaction orders and activation energies (Table 2). Additionally, it was observed that the catalyst aging at 240 °C and 260 °C at equilibrium conversion at 50 bar results in a higher active Zn coverage, 13.1% and 19.9% respectively, highly likely due to a higher CO fraction during catalyst aging.
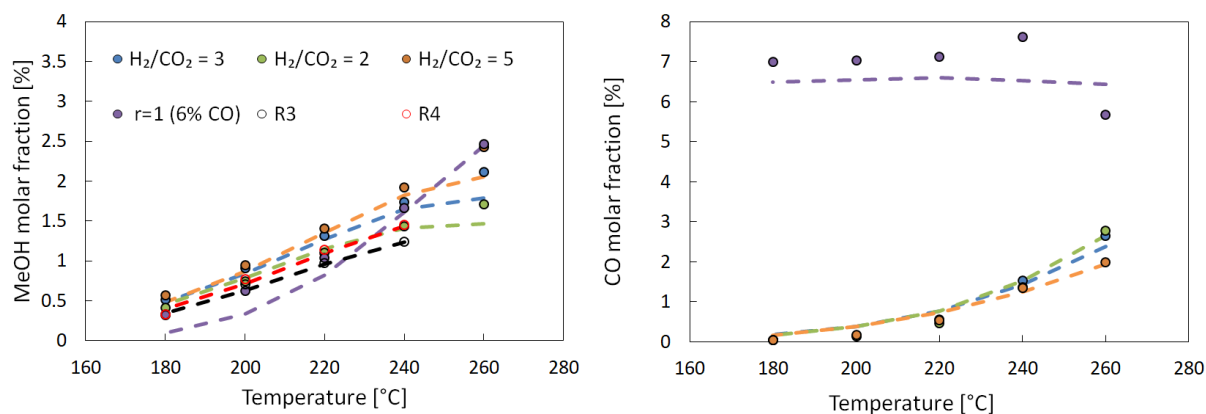

Figure 8: Parity plots for MeOH and CO molar fraction for all used catalysts. Circles represent experimental data and dashed lines the model results.

Table 3: Concentrations of active sites on CuZnAl catalysts.

c (Cu) [mol/L][1]	c (Zn) [mol/L]	coverage (Zn) [%]

R3	0.1387	0.0209^2	13.1^2 (observed 23^3)
R4	0.2999	0.0229^3	7.1^3
R9	0.0966	0.024^2	19.9^2

[1]obtained by N_2O PSO, [2] fitted concentration, [3] obtained from $ECSF_{Cu}$

To demonstrate the effect of the active Zn coverage on catalysis we calculated the activity at the same conditions as were used for the catalytic tests using a commercial CuZnAl catalyst by Kuld et al.[37] (130 °C, 1 bar, $H_2/CO_2/CO$=64/18/18, differential conditions) for the catalyst at constant total number of active sites (Cu+Zn) and different Zn coverage (Figure 9a). We observed that MeOH synthesis parabolically increases up to 0.4 Zn coverage and then starts to decline, similarly as is observed in the reference case. The temperature increase from 130 °C to 240 °C results in a shift of the maximum activity to 0.1 Zn coverage and a less steep decrease of activity, due to lower occupation of Cu sites by reaction intermediates, leaving free sites for H_2 activation. By increasing the pressure from 1 bar to 20 bar at 240 °C the optimal Zn coverage shifts to 0.3, which is a result of the higher rate of H_2 activation due to increased H_2 partial pressure, leading to a better utilization of active Zn sites. Figure 9b depicts the temperature dependence of reaction intermediates' coverages at 20 bar and $H_2/CO_2/CO$=64/18/18. We can observe that the most abundant carbon based reaction intermediates are methoxy and formate which are in line with the fact that formate species are regularly found as the most abundant reaction intermediates on CuZn systems.[17,59]
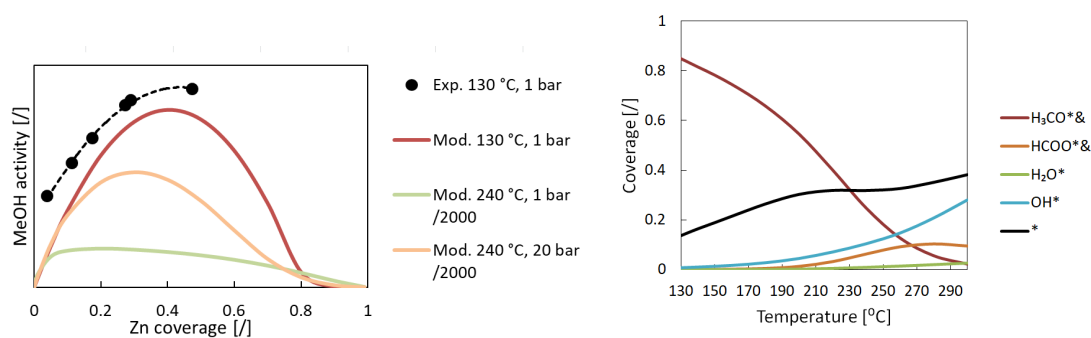

Figure 9: a) Effect of the Zn coverage on the catalytic activity (blue line), model correction by accounting aggregation of Zn atoms (red line) and reference activity of the CZA catalyst Kuld et al. b) Zn active sites

(labeled by *) are almost entirely covered by reaction intermediates at various temperatures (20 bar, $H_2/CO_2=3$, GHSV 40.000 h^{-1}).

We can observe that the activity of reference case in Figure 9a at zero Zn coverage does not converge to 0 activity but to around the third of the maximum activity. The high activity at low coverage can be attributed to two different accounts. The first is that the contact between the Cu and ZnO phases is also active as seen with the model Cu/ZnO(0001) catalyst. Indeed, the results from the model catalyst by comparing Cu/ZnO(0001) and Zn/Cu(111) show that the normalized activities are in the same order of the activity (Figure 3). The second is the contribution of the Al_2O_3 phase, where CuAl can on the average reach 41% of the activity of the CuZnAl catalyst (Figure 1). We dismiss the activity of pure Cu as a relevant contribution, since it contributes on the average only 7% to the activity. Such low Zn coverages are however not relevant to the industrial systems and the two site model can adequately describe the catalytic interplay between Cu and Zn abundance of the commercial system.

4. Conclusions

In this study we systematically and quantitively determine the various contributions to the CuZnAl catalyst activity and use the obtained knowledge to prepare a multisite microkinetic model for CO_2 reduction. The amount of catalytically active ZnO_X on copper surface has the highest influence on the activity. On the commercial CuZnAl catalyst, the CO and/or MeOH increase the ZnO_X coverage while H_2O promotes ZnO particle growth resulting in a partially inactive ZnO_X layer near the ZnO particles, while the nature of active sites remains almost unchanged when comparing apparent reaction orders and activation energies. We observed an increased methanol synthesis activity (normalized to Cu surface sites) with the uncovering of Al_2O_3 from Cu, indicating a steric hindrance of Cu-Zn active sites. Based on the fact that the catalytic active Zn sites need to be surrounded by Cu atoms, which are necessary for H_2 activation, we developed a multisite microkinetic model with Cu and Zn active sites. The model is based on experimentally measured H_2 activation kinetics and reaction rate constants obtained by DFT for the Zn/Cu(211) surface, and was optimized using the results of experiments at industrially relevant conditions. The activity trends of ZnO_X coverage variation match those of experimentally measured values providing us with a useful model, which can be further upgraded by reaction condition dependant Zn coverage as well as by incorporating Cu particle growth and Zn overgrowth during deactivation or adding other active sites due to the catalyst modification.

CRediT authorship contribution statement

Anže Prašnikar: Conceptualization, Methodology, Validation, Formal analysis, Investigation, Resources, Data Curation, Writing - Original Draft, Visualization. **Damjan Lašič Jurković:** Resources, Formal analysis, Software, Writing - Original Draft, Writing - Review & Editing. **Blaž Likozar:** Conceptualization, Writing - Review & Editing, Supervision, Funding acquisition.

Declaration of Competing Interest

The authors declare that they have no known competing financial interests or personal relationships that could have appeared to influence the work reported in this paper.

Acknowledgments

5. References

[1]   A. Varone, M. Ferrari, Power to liquid and power to gas: An option for the German Energiewende, Renew. Sustain. Energy Rev. 45 (2015) 207–218. doi:10.1016/j.rser.2015.01.049.

[2]   S. Kattel, P. Liu, J.G. Chen, Tuning Selectivity of CO2 Hydrogenation Reactions at the Metal/Oxide Interface, J. Am. Chem. Soc. 139 (2017) 9739–9754. doi:10.1021/jacs.7b05362.

[3]   H. Bahruji, M. Bowker, G. Hutchings, N. Dimitratos, P. Wells, E. Gibson, W. Jones, C. Brookes, D. Morgan, G. Lalev, Pd/ZnO catalysts for direct CO2 hydrogenation to methanol, J. Catal. 343 (2016) 133–146. doi:10.1016/j.jcat.2016.03.017.

[4]   Y. Hartadi, D. Widmann, R.J. Behm, CO2 hydrogenation to methanol on supported Au catalysts under moderate reaction conditions: Support and particle size effects, ChemSusChem. 8 (2015) 456–465. doi:10.1002/cssc.201402645.

[5]   R. van den Berg, G. Prieto, G. Korpershoek, L.I. van der Wal, A.J. van Bunningen, S. Lægsgaard-Jørgensen, P.E. de Jongh, K.P. de Jong, Structure sensitivity of Cu and CuZn catalysts relevant to industrial methanol synthesis, Nat. Commun. 7 (2016) 13057. doi:10.1038/ncomms13057.

[6]   T. Fujitani, J. Nakamura, The effect of ZnO in methanol synthesis catalysts on Cu dispersion and the specific activity, Catal. Letters. 56 (1998) 119–124. doi:10.1023/A:1019000927366.

[7]   M.M. Günter, T. Ressler, B. Bems, C. Büscher, T. Genger, O. Hinrichsen, M. Muhler, R. Schlögl, Implication of the microstructure of binary Cu/ZnO catalysts for their catalytic activity in methanol synthesis, Catal. Letters. 71 (2001) 37–44. doi:10.1023/A:1016696022840.

[8]   J.. Friedrich, M.S. Wainwright, D.J. Young, Methanol Synthesis over Raney Copper-Zinc Catalysts, I. Activities and Surface Properties of Fully Extracted Catalysts, J. Catal. 80 (1983) 1–13. doi:10.1016/0021-9517(83)90223-3.

[9]   J. Schumann, M. Eichelbaum, T. Lunkenbein, N. Thomas, M.C. Álvarez Galván, R. Schlögl, M. Behrens, Promoting strong metal support interaction: Doping ZnO for enhanced activity of Cu/ZnO:M (M = Al, Ga, Mg) catalysts, ACS Catal. 5 (2015) 3260–3270. doi:10.1021/acscatal.5b00188.

[10]   M. Kurtz, H. Wilmer, T. Genger, O. Hinrichsen, M. Muhler, Deactivation of supported copper catalysts for methanol synthesis, Catal. Letters. 86 (2003) 77–80. doi:10.1023/A:1022663125977.

[11]   A. Karelovic, G. Galdames, J.C. Medina, C. Yévenes, Y. Barra, R. Jiménez, Mechanism and structure sensitivity of methanol synthesis from CO2 over SiO2-supported Cu nanoparticles, J. Catal. 369 (2019) 415–426. doi:10.1016/j.jcat.2018.11.012.

[12]   A. Karelovic, P. Ruiz, The role of copper particle size in low pressure methanol synthesis via CO2 hydrogenation over Cu/ZnO catalysts, Catal. Sci. Technol. 5 (2015) 869–881. doi:10.1039/C4CY00848K.

[13] S. Kattel, P.J. Ramirez, J.G. Chen, J.A. Rodriguez, P. Liu, Active sites for CO2 hydrogenation to methanol on Cu/ZnO catalysts, Science. 355 (2017) 1296–1299. doi:10.1126/science.aal3573.

[14] T. Fujitani, I. Nakamura, T. Uchijima, The kinetics and mechanism of methanol synthesis by hydrogenation of C02 over a Zn-deposited Cu (111) surface, 383 (1997) 4–8. doi:10.1016/S0039-6028(97)00192-1.

[15] Y. Yang, J. Evans, J. a Rodriguez, M.G. White, P. Liu, Fundamental studies of methanol synthesis from CO2 hydrogenation on Cu(111), Cu clusters, and Cu/ZnO(0001)., Phys. Chem. Chem. Phys. 12 (2010) 9909–9917. doi:10.1039/c001484b.

[16] P.B. Rasmussen, M. Kazuta, I. Chorkendorff, Synthesis of methanol from a mixture of H2 and CO2 on Cu (100), Surf. Sci. 318 (1994) 267–280. doi:10.1016/0039-6028(94)90101-5.

[17] T. Koitaya, S. Yamamoto, Y. Shiozawa, Y. Yoshikura, M. Hasegawa, J. Tang, K. Takeuchi, K. Mukai, S. Yoshimoto, I. Matsuda, J. Yoshinobu, CO 2 Activation and Reaction on Zn-Deposited Cu Surfaces Studied by Ambient-Pressure X-ray Photoelectron Spectroscopy, ACS Catal. 9 (2019) 4539–4550. doi:10.1021/acscatal.9b00041.

[18] R.M. Palomino, P.J. Ram, Z. Liu, R. Hamlyn, I. Waluyo, M. Mahapatra, I. Orozco, A. Hunt, J.P. Simonovis, S.D. Senanayake, J.A. Rodriguez, P.J. Ramirez, Z. Liu, R. Hamlyn, I. Waluyo, M. Mahapatra, I. Orozco, A. Hunt, J.P. Simonovis, S.D. Senanayake, J.A. Rodriguez, Hydrogenation of CO_2 on ZnO/Cu(100) and ZnO/Cu(111) Catalysts: Role of Copper Structure and Metal − Oxide Interface in Methanol Synthesis, J. Phys. Chem. B. 122 (2018) 794–800. doi:10.1021/acs.jpcb.7b06901.

[19] Y. Yang, C.A. Mims, D.H. Mei, C.H.F. Peden, C.T. Campbell, Mechanistic studies of methanol synthesis over Cu from CO/CO2/H2/H2O mixtures: The source of C in methanol and the role of water, J. Catal. 298 (2013) 10–17. doi:10.1016/j.jcat.2012.10.028.

[20] P.L. Hansen, J.B. Wagner, S. Helveg, J.R. Rostrup-Nielsen, B.S. Clausen, Henrik, Atom-resolved imaging of dynamic shape changes in supported copper nanocrystals, Science. 295 (2002) 2053–2055. doi:10.1126/science.1069325.

[21] T. Lunkenbein, F. Girgsdies, T. Kandemir, N. Thomas, M. Behrens, R. Schlögl, E. Frei, Bridging the Time Gap: A Copper/Zinc Oxide/Aluminum Oxide Catalyst for Methanol Synthesis Studied under Industrially Relevant Conditions and Time Scales, Angew. Chemie - Int. Ed. 55 (2016) 12708–12712. doi:10.1002/anie.201603368.

[22] M. Behrens, F. Studt, I. Kasatkin, S. Kuhl, M. Havecker, F. Abild-Pedersen, S. Zander, F. Girgsdies, P. Kurr, B.L. Kniep, M. Tovar, R.W. Fischer, J.K. Norskov, R. Schlogl, The active site of methanol synthesis over Cu/ZnO/Al2O3 industrial catalysts, Science. 336 (2012) 893–897. doi:10.1126/science.1219831.

[23] L.C. Grabow, M. Mavrikakis, Mechanism of methanol synthesis on Cu through CO2 and CO hydrogenation, ACS Catal. 1 (2011) 365–384. doi:10.1021/cs200055d.

[24] F. Studt, M. Behrens, E.L. Kunkes, N. Thomas, S. Zander, A. Tarasov, J. Schumann, E. Frei, J.B. Varley, F. Abild-Pedersen, J.K. Nørskov, R. Schlögl, The Mechanism of CO and CO2 Hydrogenation to Methanol over Cu-Based Catalysts, ChemCatChem. 7 (2015) 1105–1111. doi:10.1002/cctc.201500123.

[25] Q.-L. Tang, W.-T. Zou, R.-K. Huang, Q. Wang, X.-X. Duan, Effect of the components' interface on the synthesis of methanol over Cu/ZnO from CO2/H2 : a microkinetic analysis based on DFT + U calculations, Phys. Chem. Chem. Phys. Phys. Chem. Chem. Phys. 17 (2015) 7317–7333. doi:10.1039/c4cp05518g.

[26] Y.-F. Zhao, Y. Yang, C. Mims, C.H.F. Peden, J. Li, D. Mei, Insight into methanol synthesis from CO2 hydrogenation on Cu(111): Complex reaction network and the effects of H2O, J. Catal. 281 (2011) 199–211. doi:10.1016/j.jcat.2011.04.012.

[27] M. Huš, V.D.B.C. Dasireddy, N. Strah Stefančič, B. Likozar, Mechanism, kinetics and thermodynamics of catalytic carbon dioxide hydrogenation to methanol on Cu/ZnAl2O4 spinel-type catalyst, Appl. Catal. B Environ. 207 (2017) 267–278. doi:10.1016/j.apcatb.2017.01.077.

[28] M. Huš, D. Kopač, N. Strah Štefančič, D. Lašič Jurković, V.D.B.C. Dasireddy, B. Likozar, Unravelling the mechanisms of CO2 hydrogenation to methanol on Cu-based catalysts using first-principles multiscale modelling and experiments, Catal. Sci. Technol. 7 (2017) 5900–5913. doi:10.1039/c7cy01659j.

[29] X. Fan, Q. Tang, X. Zhang, T. Zhang, Q. Wang, X. Duan, Applied Surface Science Comprehensive theoretical analysis of the influence of surface alloying by zinc on the catalytic performance of Cu (110) for the production of methanol from CO2 selective hydrogenation : Part 1 – Thermochemical aspects, Appl. Surf. Sci. 469 (2019) 841–853. doi:10.1016/j.apsusc.2018.11.038.

[30] G. Prieto, S. Beijer, M.L. Smith, M. He, Y. Au, Z. Wang, D.A. Bruce, K.P. de Jong, J.J. Spivey, P.E. de Jongh, Design and Synthesis of Copper-Cobalt Catalysts for the Selective Conversion of Synthesis Gas to Ethanol and Higher Alcohols, Angew. Chemie. 126 (2014) 6515–6519. doi:10.1002/ange.201402680.

[31] A.J. Medford, A.C. Lausche, B. Temel, N.C. Schjødt, J.K. Nørskov, F. Studt, Activity and Selectivity Trends in Synthesis Gas Conversion to Higher Alcohols, Top. Catal. 57 (2014) 135–142. doi:10.1007/s11244-013-0169-0.

[32] F. Studt, I. Sharafutdinov, F. Abild-pedersen, C.F. Elkjær, J.S. Hummelshøj, S. Dahl, I. Chorkendorff, J.K. Nørskov, Discovery of a Ni-Ga catalyst for carbon dioxide reduction to methanol, Nat. Chem. 6 (2014) 320–324. doi:10.1038/nchem.1873.

[33] A. Prašnikar, A. Pavlišič, F. Ruiz-Zepeda, J. Kovač, B. Likozar, Mechanisms of Copper-Based Catalyst Deactivation during CO2 Reduction to Methanol, Ind. Eng. Chem. Res. 58 (2019) 13021–13029. doi:10.1021/acs.iecr.9b01898.

[34] M. Sano, T. Adaniya, T. Fujitani, J. Nakamura, Oxidation of a Zn-deposited Cu (1 1 1) surface studied by XPS and STM, Surf. Sci. 514 (2002) 261–266. doi:10.1016/S0039-6028(02)01639-4.

[35] J.-D. Grunwaldt, A.M. Molenbroek, N.-Y. Topsøe, H. Topsøe, B.S. Clausen, In Situ Investigations of Structural Changes in Cu/ZnO Catalysts, J. Catal. 194 (2000) 452–

460. doi:10.1006/jcat.2000.2930.

[36] T. Lunkenbein, J. Schumann, M. Behrens, R. Schlçgl, M.G. Willinger, Formation of a ZnO Overlayer in Industrial Cu/ZnO/Al2O3 Catalysts Induced by Strong Metal – Support Interactions, Angew. Chemie - Int. Ed. 54 (2015) 4544–4548. doi:10.1002/anie.201411581.

[37] S. Kuld, M. Thorhauge, H. Falsig, C.F. Elkjær, S. Helveg, I. Chorkendorff, J. Sehested, Quantifying the promotion of Cu catalysts by ZnO for methanol, Science. 352 (2016) 2920. doi:10.1002/9783527610044.hetcat0148.

[38] H. Wilmer, T. Genger, O. Hinrichsen, The interaction of hydrogen with alumina-supported copper catalysts: A temperature-programmed adsorption/temperature-programmed desorption/isotopic exchange reaction study, J. Catal. 215 (2003) 188–198. doi:10.1016/S0021-9517(03)00003-4.

[39] P.Y. Lanfrey, Z. V. Kuzeljevic, M.P. Dudukovic, Tortuosity model for fixed beds randomly packed with identical particles, Chem. Eng. Sci. 65 (2010) 1891–1896. doi:10.1016/j.ces.2009.11.011.

[40] R. Dias, J.A. Teixeira, M. Mota, A. Yelshin, Tortuosity variation in a low density binary particulate bed, Sep. Purif. Technol. 51 (2006) 180–184. doi:10.1016/j.seppur.2006.01.010.

[41] Y. Slotboom, M.J. Bos, J. Pieper, V. Vrieswijk, B. Likozar, S.R.A. Kersten, D.W.F. Brilman, Critical assessment of steady-state kinetic models for the synthesis of methanol over an industrial Cu/ZnO/Al2O3 catalyst, Chem. Eng. J. 389 (2020) 124181. doi:10.1016/j.cej.2020.124181.

[42] D. Lašič Jurković, CERRES, (2020). www.cerres.org.

[43] T. Fujitani, M. Saito, The role of metal oxides in promoting a copper catalyst for methanol synthesis, Catal. Letters. 25 (1994) 271–276. doi:10.1007/BF00816307.

[44] M. Saito, J. Wu, K. Tomoda, I. Takahara, K. Murata, Effects of ZnO contained in supported Cu-based catalysts on their activities for several reactions, Catal. Letters. 83 (2002) 1–4. doi:10.1023/A:1020693226903.

[45] M. Behrens, S. Zander, P. Kurr, N. Jacobsen, J. Senker, G. Koch, T. Ressler, R.W. Fischer, R. Schlögl, Performance improvement of nanocatalysts by promoter-induced defects in the support material: Methanol synthesis over Cu/ZnO:Al, J. Am. Chem. Soc. 135 (2013) 6061–6068. doi:10.1021/ja310456f.

[46] J. Nakamura, Y. Choi, T. Fujitani, On the issue of the active site and the role of ZnO in Cu/ZnO methanol synthesis catalysts, Top. Catal. 22 (2003) 227–285. doi:10.1023/A:1023588322846.

[47] M.B. Fichtl, D. Schlereth, N. Jacobsen, I. Kasatkin, J. Schumann, M. Behrens, R. Schlögl, O. Hinrichsen, Kinetics of deactivation on Cu/ZnO/Al2O3 methanol synthesis catalysts, Appl. Catal., A. 502 (2015) 262–270. doi:10.1016/j.apcata.2015.06.014.

[48] S. Natesakhawat, J.W. Lekse, J.P. Baltrus, P.R. Ohodnicki, B.H. Howard, X. Deng, C. Matranga, Active sites and structure-activity relationships of copper-based catalysts for carbon dioxide hydrogenation to methanol, ACS Catal. 2 (2012) 1667–1676.

doi:10.1021/cs300008g.

[49]   S. Kuld, C. Conradsen, P.G. Moses, I. Chorkendorff, J. Sehested, Quantification of zinc atoms in a surface alloy on copper in an industrial-type methanol synthesis catalyst, Angew. Chemie - Int. Ed. 53 (2014) 5941–5945. doi:10.1002/anie.201311073.

[50]   T. Fujitani, T. Matsuda, Y. Kushida, S. Ogihara, T. Uchijima, J. Nakamura, Creation of the active site for methanol synthesis on a Cu/SiO2 catalyst, Catal. Letters. 49 (1997) 175–179. doi:10.1023/A:1019069708459.

[51]   K. Hashimoto, S. Ogawa, S. Shimodaira, Dezincification of Alpha Brass, Trans. Japan Inst. Met. 4 (1963) 42–45. doi:10.2320/matertrans1960.4.42.

[52]   M. Saber, T.T. Huu, C. Pham-Huu, D. Edouard, Residence time distribution, axial liquid dispersion and dynamic-static liquid mass transfer in trickle flow reactor containing β-SiC open-cell foams, Chem. Eng. J. 185–186 (2012) 294–299. doi:10.1016/j.cej.2012.01.045.

[53]   D.K. Kim, E. Iglesia, Isotopic and kinetic assessment of the mechanism of CH3OH-H 2O catalysis on supported copper clusters, J. Phys. Chem. C. 112 (2008) 17235–17243. doi:10.1021/jp8062178.

[54]   O. Hinrichsen, T. Genger, M. Muhler, Probing the Elementary Steps of the Water-Gas Shift Reaction over Cu/ZnO/Al2O3 with Transient Experiments, Stud. Surf. Sci. Catal. 130 (2000) 3825–3830. doi:10.1016/S0167-2991(00)80619-9.

[55]   J. Yoshihara, C.T. Campbell, Methanol synthesis and reverse water-gas shift kinetics over Cu(110) model catalysts: Structural sensitivity, J. Catal. 161 (1996) 776–782. doi:10.1006/jcat.1996.0240.

[56]   P. Wu, B. Yang, Significance of Surface Formate Coverage on the Reaction Kinetics of Methanol Synthesis from CO2 Hydrogenation over Cu, ACS Catal. 7 (2017) 7187–7195. doi:10.1021/acscatal.7b01910.

[57]   E. Maestri, M., Vlachos, D.G., Beretta, A., Groppi, G. and Tronconi, A C1 microkinetic model for methane conversion to syngas on Rh/Al2O3, AIChE J. 59 (2012) 215–228. doi:10.1002/aic.

[58]   N. Park, M.J. Park, Y.J. Lee, K.S. Ha, K.W. Jun, Kinetic modeling of methanol synthesis over commercial catalysts based on three-site adsorption, Fuel Process. Technol. 125 (2014) 139–147. doi:10.1016/j.fuproc.2014.03.041.

[59]   I. Nakamura, H. Nakano, T. Fujitani, T. Uchijima, J. Nakamura, Evidence for a special formate species adsorbed on the Cu – Zn active site for methanol synthesis, Surf. Sci. 404 (1998) 92–95. doi:10.1016/S0039-6028(97)00910-2.